Computational Modeling and Analysis of Host–Parasite Dynamics Using the Homotopy Analysis Method: A Case Study in Aquaculture Systems

M.Rasi [a], A. Marimuthu[b], L.Rajendran [b*]

[a] PG & Research Department of Mathematics A.P.C. Mahalaxmi College for Women, Thoothukudi
[b] Department of Mathematics, AMET university, Chennai-603112

Abstract

This study presents a computational framework for modeling host–parasite interactions, specifically focusing on the dynamics between *Argulus foliaceus* and trout in aquaculture systems. A system of three coupled nonlinear ordinary differential equations is developed to describe the temporal evolution of host fish, attached parasites, and free-living parasite populations. To obtain approximate analytical solutions, the homotopy analysis method (HAM)—a powerful semi-analytical technique for solving nonlinear systems—is implemented. The derived solutions are rigorously compared with numerical simulations, exhibiting strong concordance and confirming the robustness and precision of the HAM approach. Sensitivity analysis is conducted to identify key parameters—such as host birth rate, parasite attachment rate, and mortality rate—that critically influence system behavior. The computational methodology demonstrated here not only facilitates efficient simulation and analysis of biologically complex systems but also serves as a foundation for future extensions involving spatio-temporal modeling or stochastic processes. This work underscores the potential of advanced analytical algorithms in enhancing decision-making and system control in computational biology and aquaculture management..

Keywords: Host–parasite dynamics, Homotopy analysis method (HAM), Nonlinear differential equations, Computational modelling, Aquaculture systems, Sensitivity analysis

1. Introduction

Argulus foliaceus, commonly known as the fish louse, is a large ectoparasite that significantly impacts commercially important fish species such as rainbow trout (*Oncorhynchus mykiss*) and brown trout (*Salmo trutta*) in stillwater fisheries (Pasternak et al., 2000; Oktener, 2006). Infestations by this parasite reduce fish quality and catchability, leading to reputational damage and substantial economic losses for aquaculture operations (McPherson, 2011). Parasites like *A. foliaceus* extract nutrients from their hosts, often compromising host health and increasing susceptibility to environmental stressors (Hakalahti,

2005; Rameen Atique et al., 2024). While parasite infestations rarely cause mass fish mortalities independently, they exacerbate existing stress conditions such as overcrowding, temperature fluctuations, and deteriorating water quality, gradually leading to increased fish morbidity and mortality (Bunkley-Williams et al., 1994).

Current control strategies against *A. foliaceus* rely heavily on chemical treatments and physical interventions, which are frequently expensive, ecologically disruptive, and only partially effective. Persistent infestations despite frequent treatments highlight the need for a deeper understanding of parasite-host interactions (McPherson, 2011). Computational modeling has emerged as a powerful tool in this context. Several studies (e.g., Dobson et al., 1992) have developed nonlinear ordinary differential equation (ODE)-based models to investigate the dynamics of fish-parasite interactions. These models integrate ecological parameters such as host density, parasite load, fishing pressure, and stocking strategies to simulate system behavior under varied conditions.

In particular, the work of McPherson et al. (2012) introduced a model capturing the host–parasite dynamics in trout fisheries, incorporating catchability reduction due to parasitic load and different management scenarios. However, most of these models are solved numerically, with limited availability of analytical insights into the system's behavior.

This study aims to address this gap by deriving approximate analytical solutions for the coupled nonlinear differential equations that govern the population dynamics of host fish, attached parasites, and free-living parasite stages. We apply the Homotopy Analysis Method (HAM), a semi-analytical technique known for its flexibility and robustness in solving nonlinear systems. The analytical expressions derived here facilitate deeper insight into the time-dependent behavior of the host–parasite system and provide a computational framework that can inform decision-making in aquaculture management and disease mitigation strategies.

2. Mathematical formulation of the problem

To analyze the dynamics of parasitic infestation in aquaculture systems, we propose a nonlinear dynamical model representing the interactions among three key populations: the healthy trout hosts, the attached *Argulus foliaceus* parasites, and the free-living parasitic stages (e.g., metanauplii). The model, originally conceptualized by McPherson et al. (2012), is based

on a system of coupled nonlinear ordinary differential equations (ODEs), capturing the time evolution of each subpopulation.Let H(t) denote the number of healthy (uninfected) host fish at time t, P(t) the population of parasites attached to hosts, and W(t) the population of free-living parasite stages. The dynamics of the system are governed by the following equations:

$$\frac{dH(t)}{dt} = s(H) - Hc(H,P) - \alpha P \tag{1}$$

$$\frac{dP(t)}{dt} = \beta HW - \mu P - Pc(H,P) - \alpha P(1 + kP/H) \tag{2}$$

$$\frac{dW(t)}{dt} = \lambda P - dW - \beta HW \tag{3}$$

Where H(t) is population of healthy (uninfected) host fish at time *t,* I(t) is population of infected fish (with attached parasites) at time *t*, P(t)is population of free-living parasites at time *t*. The parameters α and β represent parasite-induced mortality and the rate at which free-living parasite stages attach to the fish, respectively. Here, μ is the mortality rate of attached parasites, while λ and d represent the birth and mortality rates of the free-living parasite stages, respectively.

The nonlinear term $\alpha P(1 + kP/H)$ accounts for density-dependent parasite-induced mortality, where k controls the degree of clustering of parasites across the host population, as originally formulated by Anderson et al. (1978).This system exhibits rich nonlinear behavior due to the coupling of multiplicative interaction terms (e.g., βHW), nonlinear mortality, and nontrivial catchability dynamics. A schematic diagram of the interaction network is presented in **Fig. 1**, illustrating the biological and computational structure of the system.

From a computational perspective, the model provides a robust framework for simulating host–parasite population dynamics, validating numerical solvers, and applying analytical approximation methods such as the Homotopy Analysis Method (HAM). The system serves as a testbed for nonlinear system analysis, stability evaluation, and control strategies in biologically inspired computational modelling.

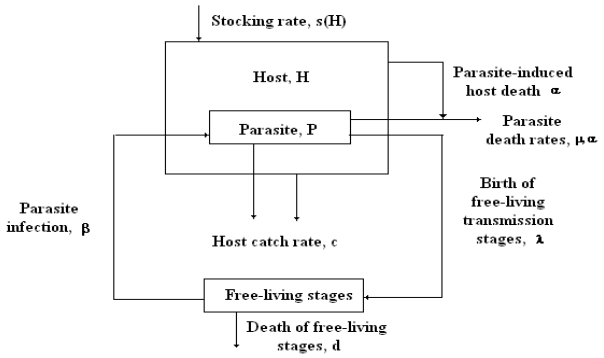

Fig.1. Compartmental Model of Parasite Transmission Dynamics

2.1. Baseline model (Constant catch rate)

In this case $s(H) = aH$ and $c(H,P) = c$. This model is included here to show the impact of the reduction in capture on a well-known model, and also to provide a point of departure for the other models presented in this paper. In this model, the rate equations become as follows (McPherson et al.2012) :

$$\frac{dH(t)}{dt} = (a-c)H - \alpha P \tag{4}$$

$$\frac{dP(t)}{dt} = \beta HW - (\mu + \alpha + c)P - \alpha k\frac{P^2}{H} \tag{5}$$

$$\frac{dW(t)}{dt} = \lambda P - dW - \beta HW \tag{6}$$

where H, P and W denotes size of fish population, attached parasite and number of free-living parasite stages respectively and $a, c, \alpha, \beta, \mu, \lambda, d$ and k denotes birth rate of fish, capture rate, increased host mortality due to parasite, rate of attachment, mortality of attached stages, birth rate of parasites, mortality of free-living stages and parameter of the negative binomial distribution which measures inversely the degree of aggregation of parasites within the host population respectively.

The initial conditions are:

$$H(t=0) = 1,\ P(t=0) = 1, W(t=0) = 1 \tag{7}$$

The system has equilibrium at

$$H^* = \frac{d\gamma}{\beta(\lambda-\gamma)}, P^* = \frac{H^*}{\alpha}(a-c), W^* = \frac{\gamma}{\beta}(a-c) \tag{8}$$

Liao (1992,2007) proposed a powerful analytical method (HAM)for solving nonlinear problems. Unlike all perturbation and non-perturbative techniques, the this method (Domairry,2009, Liao, 2010, Sohouli, 2010, Mastroberardino, 2011) provides a convenient way to control and adjust the convergent region and rate of approximation series when necessary. Briefly speaking, this method has the following advantages: It is valid even if a given nonlinear problem does not contain any small/significant parameters at all; It can be employed to efficiently approximate a nonlinear problem by choosing different base functions.

More and more researchers have been successfully applying this method to various nonlinear problems in science and engineering. In this paper, we employ HAM to solve the nonlinear differential equations (Eqns. (4) to (6)). The basic concept of the homotopy analysis method is given in Appendix A.

3. Result and Discussion of Baseline model

By solving equations (4) to (6), using the homotopy analysis method (see Appendix -B), we can obtain the following new approximate expression for the population of fish, attached parasite and number of free-living parasites as follows:

$$H(t) = e^{mt} - \frac{h\alpha}{(\gamma+\alpha+a)}\left[e^{-nt} - e^{mt}\right] \tag{9}$$

$$P(t) = e^{-nt} - \frac{h\beta}{(m+n-d)}\left[e^{(m-d)t} - e^{-nt}\right] - \frac{h\alpha k}{(\mu+\alpha+a)}\left[e^{-(2n+m)t} - e^{-nt}\right] \tag{10}$$

$$W(t) = e^{-dt} + \frac{h\lambda}{(n-d)}\left[e^{-nt} - e^{-dt}\right] + \frac{h\beta}{m}\left[e^{(m-d)t} - e^{-dt}\right] \tag{11}$$

Given that $m = (a-c)$ and $n = (\mu+\alpha+c)$, and it is specified that $a<<c$.

Since $a<<c$, the mortality rate of attached parasites is given by $m=a-c<0$, indicating a net loss or decline in the attached parasite population over time

3.1 Numerical simulation

The nonlinear equations (Eqns. (4) - (6)) are solved numerically. To show the efficiency of the present method, our result is compared with the numerical solution. The function ode45 (Range-Kutta Method) in Matlab software(Rasi et al.2013) , a function of solving the initial

value problem, is used to solve the Eqns. (4) - (6) numerically. The numerical results are compared with the analytical solution obtained using the HAM method in Figs (2) – (8).

3.2. **Effect of the parameters**

Equations (9), (10) and (11) are the new and simple analytical expressions of the fish populations, attached parasite and free-living parasite for all values of parameters.

2(a) 2(b)

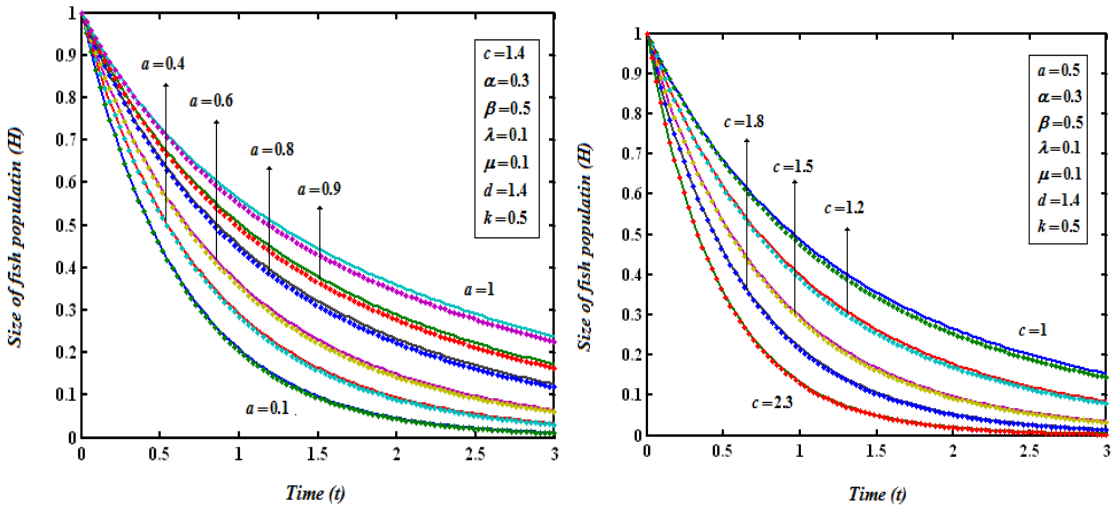

Fig.2 (a,b). Effect of the parameter *a* (birth rate of fish) and c (capture rate) on fish population using eqn.(9). Solid lines: analytical; dotted lines: numerical**.**

Figure 2(a,b) illustrates the impact of two key parameters birth rate of fish (*a*) and capture rate by parasites (*c*) on the size of the fish population H(t) over time, using both analytical and numerical approaches. The Fig.2(a) shows that as the birth rate *a* increases from 0.1 to 1.0, the fish population decreases at a slower rate. Higher values of *a* contribute to sustaining the population for a longer duration by compensating for losses due to parasitism and natural death. This indicates that a higher reproductive rate acts as a buffer against population decline, helping to maintain ecological balance even in the presence of parasitic threats.

The Fig 2(b) demonstrates the effect of varying the capture rate c, where increasing c from 1.0 to 2.3 leads to a more rapid decline in the fish population. This implies that a higher parasitic burden significantly reduces fish numbers over time. The graph clearly shows that the fish population is highly sensitive to changes in parasitic intensity, emphasizing the need for controlling parasite levels in aquatic systems. Both panels reveal excellent agreement between the analytical and numerical results, validating the accuracy of the proposed model and its potential use in predicting and managing fish population dynamics in parasitized environments.

3(a) 3(b)

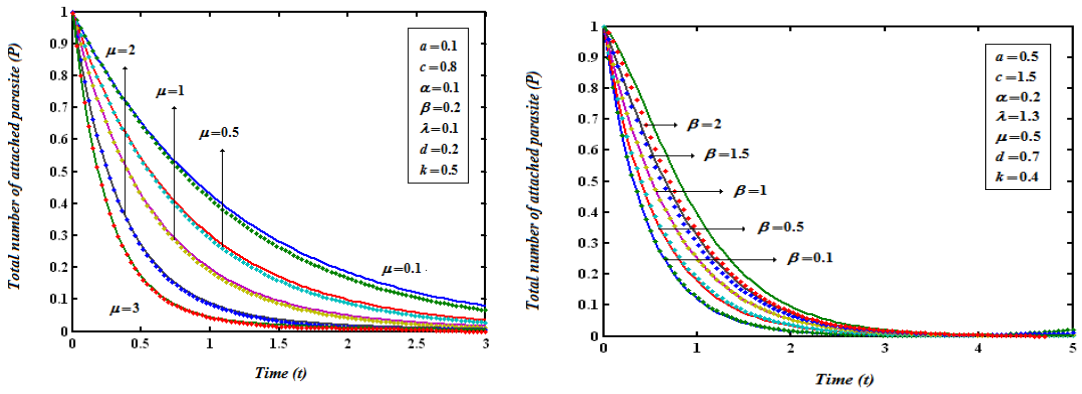

Fig. 3(a, b). Effect of (a) μ (mortality of attached stages) and (b) λ (attachment rate) on attached parasites using Eq. (10). Solid lines: analytical; dotted lines: numerical**.**

Figures 3(a) and 3(b) collectively illustrate the time-dependent behavior of the total number of attached parasites P(t) under the influence of varying parameters μ and β, respectively. In Figure 3(a), the parameter μ is varied while keeping other parameters constant. As μ increases, the decay of P(t) becomes more rapid, indicating that a higher μ which likely represents the detachment or natural mortality rate of parasites accelerates the reduction of parasite load on the host. This suggests that enhancing mechanisms associated with parasite removal (e.g., host immune response or detachment) leads to faster elimination of parasites from the system.

In contrast, Figure 3(b) demonstrates the effect of the parameter β on parasite dynamics. Increasing β also results in a faster decline of P(t), though this parameter may represent an external control factor such as treatment strength or environmental pressure. The curves show that a higher β significantly enhances the reduction rate of parasite attachment, similar to the role of μ in Figure 3(a). Together, these figures highlight the critical influence of both internal (biological) and external (intervention-based) parameters in effectively managing parasite populations, with both μ and β serving as key levers for controlling infection spread over time.

Figures 4(a) and 4(b) illustrate the dynamic behavior of the number of free-living parasites W(t) over time, under the influence of different model parameters—specifically, the diffusion coefficient d in Fig. 4(a) and the interaction rate λ in Fig. 4(b). Both figures consistently show a decay in the parasite population with time, indicating a natural or environmentally driven decline process. However, the rate and extent of this decay vary significantly depending on the values of d and λ.

In Fig. 4(a), increasing the diffusion parameter d accelerates the decay of W(t). This suggests that higher diffusion may enhance the dispersion or mortality of parasites in the environment, leading to a faster depletion of the free-living population. For instance, when d=4, the parasite count rapidly declines, whereas for smaller d values such as 1 or 1.5, the decay is more gradual, indicating lower environmental dissipation.

4(a) 4(b)

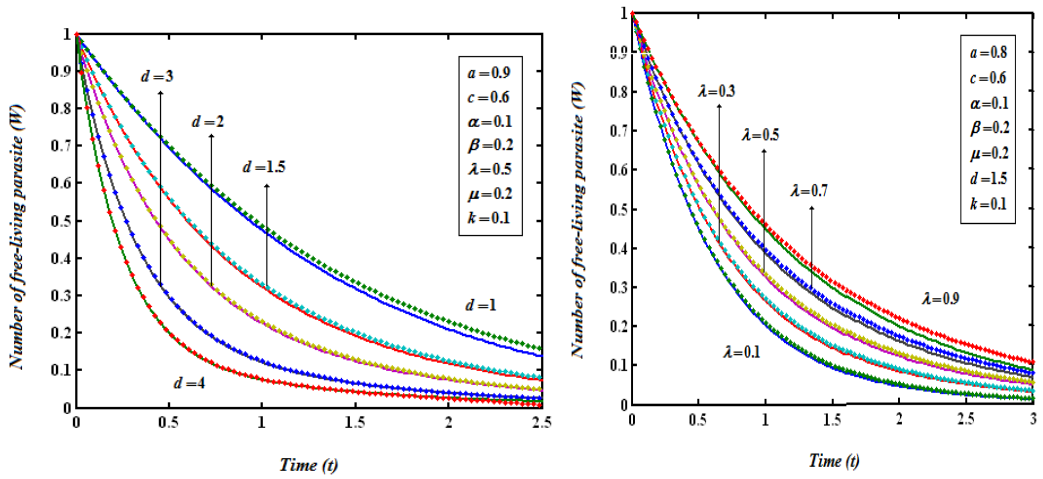

Fig. 4(a, b). Free-living parasites vs. time from Eq. (11) for varying parameter values, with other parameters fixed. Solid lines: analytical (Eq. 11); dotted lines: numerical simulation.

In Fig. 4(b), a similar trend is observed with respect to the interaction rate λ. As λ increases, the parasite population declines more swiftly. This parameter likely governs the rate at which parasites infect hosts or transition out of the free-living phase. A higher λ implies more effective host-parasite interaction, leading to a faster reduction in W(t).

Together, these figures emphasize the critical roles of both environmental (diffusion) and biological (infection or interaction) parameters in determining the persistence of free-living parasites. Effective parasite control strategies could target either increased environmental removal (via higher d) or enhanced host-parasite interaction (via higher λ) to minimize the risk of infection in aquatic ecosystems.

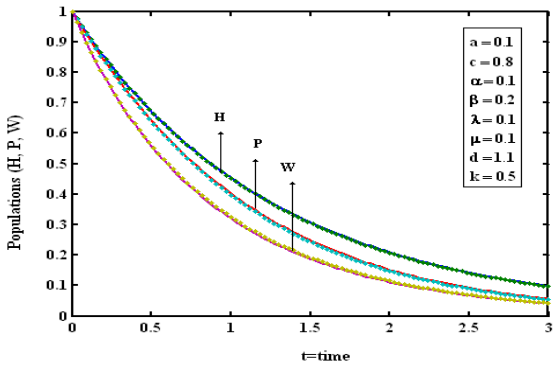

Fig.5 The population of fish H, attached parasite P and free-living parasite W versus time t for some fixed values of parameters.

Figure 5 illustrates the dynamic interaction between three populations: fish, attached parasites, and free-living parasites, as a function of time under a fixed set of parameter values. Initially, the fish population shows a gradual decline, likely due to increasing parasite load that hampers survival and reproduction. In contrast, the attached parasite population rises steadily as more parasites infect host fish. The free-living parasite population initially surges rapidly—possibly due to reproduction and lack of immediate attachment—but eventually begins to stabilize or decline as attachment opportunities or host availability decrease.

Over time, a clear interaction pattern emerges. The peak in free-living parasites precedes the rise in attached parasites, indicating a time lag between release and successful infection. Meanwhile, the fish population reaches a lower equilibrium or continues declining, reflecting the cumulative effect of parasitic pressure. This figure underscores the interconnected dynamics and time-delayed feedbacks within the host–parasite system, revealing how changes in one population influence the others over time.

4. Host–Parasite Model with Reproductive Suppression

Host–parasite interactions play a critical role in shaping the population dynamics of aquatic ecosystems, particularly in aquaculture environments where parasitic infections can significantly impair host survival and productivity. In this study, we propose a nonlinear mathematical model to describe the dynamics between a host fish population (e.g., trout) and a parasitic species (*Argulus foliaceus*), incorporating key biological mechanisms such as parasite-induced reproductive suppression and nonlinear attachment behavior. The model captures three interacting populations: the host fish, the attached parasites, and the free-living (waterborne) parasites. Unlike classical models, this formulation introduces an exponential function to represent the reduction in host fecundity as a function of parasite burden, as well as a nonlinear mortality term to reflect parasite competition and density-dependent effects. This extended framework provides a more realistic representation of host–parasite interactions and offers valuable insights for developing effective management strategies in fishery systems. Taking into account the parasite-induced reduction in capture, the rate equations in this model becomes

$$\frac{dH(t)}{dt} = (a - ce^{-\theta P/H})H - \alpha P \tag{12}$$

$$\frac{dP(t)}{dt} = \beta HW - (\mu + \alpha + ce^{-\theta P/H})P - \alpha k\frac{P^2}{H} \tag{13}$$

$$\frac{dW(t)}{dt} = \lambda P - dW - \beta HW \tag{14}$$

5. Result and Discussion of Host–Parasite interaction model

By solving the equations (12) to (14), using Homotopy analysis method (see Appendix - B) we can obtain the following new approximate expression for the population of fish, attached parasite and free-living parasite as follows:

$$H(t)=e^{mt}-\frac{h(\alpha-c\theta)}{(m+n)}\left[e^{-nt}-e^{mt}\right] \tag{15}$$

$$P(t)=e^{-nt}-\frac{h\beta}{(m+n-d)}\left[e^{(m-d)t}-e^{-nt}\right]-\frac{h(\alpha k-\theta)}{(m+n)}\left[e^{-(2n+m)}-e^{-nt}\right] \tag{16}$$

$$W(t)=e^{-dt}+\frac{h\lambda}{(n-d)}\left[e^{-nt}-e^{-dt}\right]+\frac{h\beta}{m}\left[e^{(m-d)t}-e^{-dt}\right] \tag{17}$$

Where $m=(a-c)$ and $n=(\mu+\alpha+1)$

5.1. Numerical simulation

The nonlinear boundary-value problem given by Eqs. (12)–(14) was also solved numerically in order to assess the accuracy and efficiency of our HAM-based analytic approximation. To that end, we employed MATLAB's built-in ode45 solver—which implements an adaptive Runge–Kutta method—to integrate the system as an initial-value problem over the same domain and with the identical parameter set (Matlab 6.1). Figures 12–14 overlay the numerical profiles generated by ode45 against our HAM solution: in each case, the two curves are virtually indistinguishable, confirming that the present analytic approach reproduces the high-fidelity, numerically obtained results with excellent precision.

5.2 Effect of the parameters

6(a) 6(b)

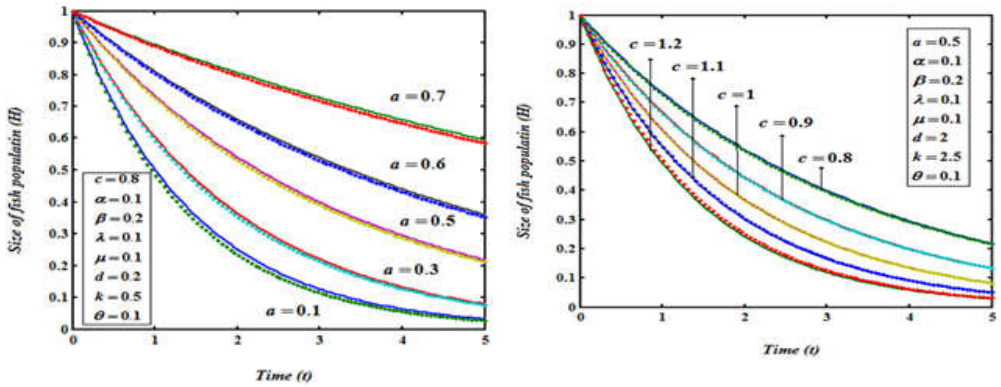

Fig. 6. Fish population size vs. time from Eq. (15) for different b and γ , representing birth and capture rates. Solid lines: analytical; dotted lines: numerical.

The size of fish population H versus the time t are plotted from Eqn. (15) for various values of a (birth rate of fish) and c (capture rate), and for some fixed values of parameters in (a) and (b) respectively. The key to the graph: Solid line represents Eqn. (15) and dotted line represents the numerical simulation

Figure 6(a) illustrates the effect of varying the fish birth rate parameter a on the size of the fish population H(t) over time, while keeping other parameters constant. It is observed that as the birth rate increases from a=0.1 to a=0.7, the rate of decline in fish population decreases significantly. For lower values of a, the fish population drops rapidly, indicating that natural reproduction is insufficient to counterbalance the losses due to mortality and harvesting. Conversely, higher values of a help sustain the population over a longer time frame, highlighting the positive influence of reproductive capacity on population survival.

Figure 6(b) explores the impact of different capture rates ccc on the fish population dynamics under fixed birth and other ecological parameters. As the capture rate increases from c=0.8 to c=1.2, the fish population declines more quickly. This trend confirms that higher harvesting pressure directly accelerates population reduction, even when the birth rate remains moderate. The results emphasize the sensitivity of fish population sustainability to the capture rate, reinforcing the importance of regulating fishing efforts to avoid overexploitation and potential collapse of the fish stock.

7(a) 7(b)

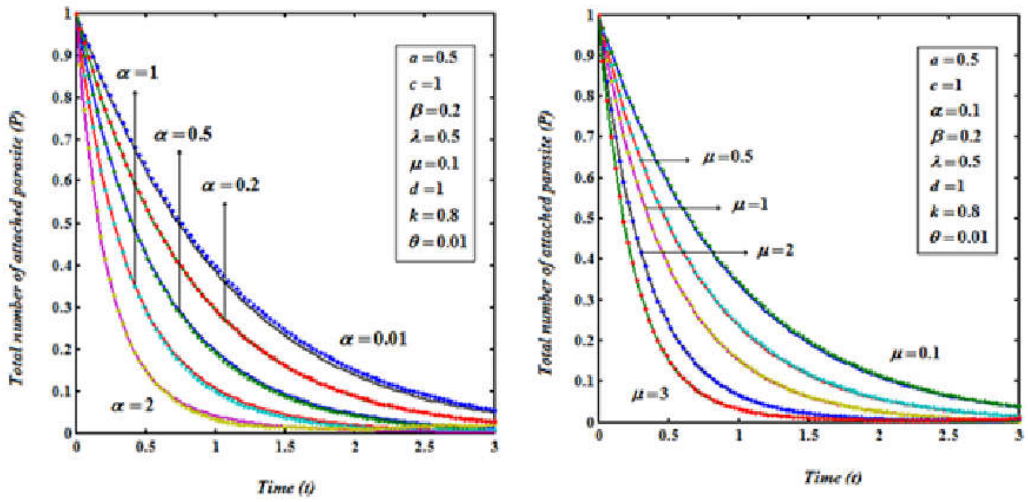

Fig. 7. Total number of attached parasites over time for varying μ and α. Solid lines: analytical solution from Eq. (16); dotted lines: numerical simulation.

Fig. 7(a) demonstrates the influence of the parameter α, representing the mortality rate of attached parasite stages, on the total number of attached parasites P(t) over time. As α

increases from 0.01 to 2, the decline in parasite population becomes more rapid. Higher values of α correspond to faster elimination of parasites, likely due to enhanced death rates at the attached stage. In contrast, when α is low, the parasite population persists for a longer duration, indicating slower mortality. These results underscore the critical role of parasite mortality in reducing parasite burden and suggest that interventions aimed at increasing parasite death rates can effectively lower infection levels over time.

Fig. 7(b) investigates the effect of the parameter μ, which represents the increased mortality of the host due to parasite infestation, on the parasite population dynamics. As μ increases from 0.1 to 3, the total number of attached parasites decreases more sharply. This pattern arises because higher host mortality indirectly reduces the parasite population by shortening the host's lifespan, thereby limiting the parasite's ability to survive and reproduce. Lower values of μ lead to slower decay in parasite numbers, indicating prolonged host viability and sustained parasite presence. This analysis highlights the importance of host–parasite interaction dynamics in determining parasite survival and can inform strategies that disrupt parasite lifecycles by enhancing host resistance or reducing host susceptibility.

8(a) 8(b)

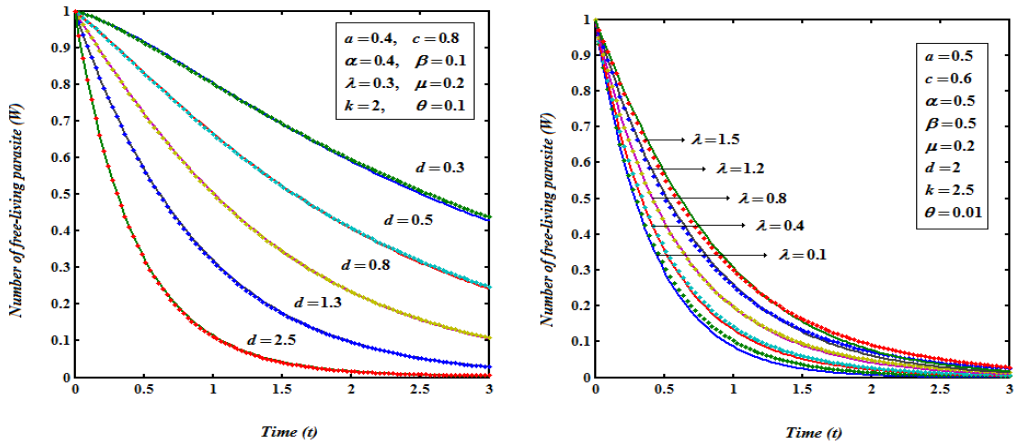

Fig. 8. Free-living parasites vs. time from Eq. (17) for different μ and β. Solid lines: analytical; dotted lines: numerical.

Fig. 8(a) illustrates the effect of the mortality rate *d* on the number of free-living parasites *H*(t) over time. As d increases from 0.3 to 2.5, the parasite population declines more rapidly. This indicates that higher mortality significantly reduces the survival duration of the free-living parasites. For instance, when *d*=2.5, the population quickly approaches zero, while at lower values like *d*=0.3, the decay is much slower. Thus, the mortality rate plays a crucial role in determining the persistence of parasites in the environment, with higher values leading to faster population extinction.

In contrast, Fig. 8(b) demonstrates the impact of the birth rate λ on the parasite population dynamics. As λ increases from 0.1 to 1.5, the number of parasites declines more slowly, suggesting that higher birth rates promote longer survival of the population. At low λ, the population decays quickly, whereas higher values of λ effectively counterbalance the mortality and maintain the population for a longer period. This highlights the importance of the reproduction rate in sustaining free-living parasites, even under conditions of high mortality or environmental stress.

6. Conclusions and Future work

In this study, we developed and analyzed a nonlinear system of ordinary differential equations modeling the dynamic interactions among host fish, attached parasites (*Argulus foliaceus*), and their free-living stages. The model captures key biological mechanisms such as parasite-induced suppression of host reproduction and nonlinear attachment dynamics. To solve the resulting strongly nonlinear system, we employed the Homotopy Analysis Method (HAM)—a powerful semi-analytical technique that avoids traditional linearization or perturbation assumptions and is particularly well-suited for high-complexity models.

The derived analytical expressions offer valuable insights into the transient behavior of the system and the sensitivity of population dynamics to key parameters, including attachment rate, mortality coefficients, and parasite burden. The effectiveness of the HAM framework was confirmed through numerical simulations carried out in Scilab/MATLAB, which demonstrated strong consistency between analytical approximations and numerical results. This synergy between analytical modeling and computational validation establishes a robust hybrid methodology for addressing nonlinear systems in biological and ecological contexts.

From a computational standpoint, this work underscores the utility of symbolic and numerical hybrid algorithms for solving real-world nonlinear dynamical systems. The modeling framework and solution strategy presented here can serve as a foundation for developing simulation tools and predictive software in fields such as ecological modeling, epidemiological forecasting, and complex systems analysis.

Future research directions include extending the current model to account for spatial heterogeneity using reaction–diffusion systems and integrating time-delay elements to reflect biological maturation periods. Incorporating stochastic dynamics, parameter uncertainty, and data-driven calibration would further improve the model's applicability to real-world fisheries. Additionally, the development of optimal control algorithms based on this framework could

inform sustainable parasite management strategies. These extensions would significantly enhance the versatility of the proposed computational model, enabling its application to a broader range of nonlinear systems in computational biology, applied mathematics, and artificial intelligence–driven ecological modeling.

Author Contributions Conceptualization, M.R.; methodology, A.M. and L.R.; software, M.R. and L.R.; validation, M.R. and A.M.; formal analysis, M.R and L.R.; investigation, M.R. and A.M.; resources, L.R. and M.R.;data curation, A.M. and M.R.; writing—original draft preparation, L.R. and M.R.; writing—review and editing,M.R. and A.M.; visualization, M.R. and L.R. All authors have read and agreed to the published version of the manuscript.

Funding No funds, grants, or other support was received.
Availability of data and materials Data sharing not applicable to this article as no datasets were generated or analysed during the current study.

Declarations
Conflict of interest: The authors have no financial or proprietary interests in any material discussed in this article.

References.

[1] R. M. Anderson and R. M. May, “Regulation and stability of host-parasite population interactions: I. Regulatory processes,” *J. Anim. Ecol.*, vol. 47, pp. 219–247, 1978.
[2] R. Atique, A. Saeed, and A. Haidar, “Host-parasite interactions; from co-evolutionary changes to genomic insights,” *Glob. J. Univ. Stud.*, vol. 8, pp. 81–95, 2024.
[3] L. Bunkley-Williams and E. H. Williams Jr., *Parasites of Puerto Rican freshwater sport fishes*, Dep. Nat. Environ. Resour., San Juan & Univ. Puerto Rico, Mayaguez, pp. 1–168, 1994.
[4] A. P. Dobson and P. J. Hudson, “Regulation and stability of free-living host-parasite system: *Trichostrongylus tenuis* in red grouse. II. Population models,” *J. Anim. Ecol.*, vol. 61, pp. 487–498, 1992.
[5] G. Domairry and H. Bararnia, “An approximation of the analytic solution of some nonlinear heat transfer equations: A survey by using homotopy analysis method,” *Adv. Stud. Theor. Phys.*, vol. 2, pp. 507–518, 2008.
[6] G. Domairry and M. Fazeli, “Homotopy analysis method to determine the efficiency of convective straight fins with temperature-dependent thermal conductivity,” *Commun. Nonlinear Sci. Numer. Simul.*, vol. 14, pp. 489–499, 2009.

[7] T. Hakalahti, *Studies of the life history of a parasite: A basis for effective population management*, Stud. Biol. Environ. Sci., vol. 152, pp. 1–43, 2005.
[8] S. J. Liao, *Ph.D. thesis*, Shanghai Jiao Tong University, Shanghai, 1992.
[9] S. J. Liao, *Beyond perturbation: Introduction to the homotopy analysis method*, 1st ed., Chapman & Hall/CRC Press, Boca Raton, FL, 2003.
[10] S. J. Liao, "An optimal homotopy-analysis approach for strongly nonlinear differential equations," *Commun. Nonlinear Sci. Numer. Simul.*, vol. 15, pp. 2003–2016, 2010.
[11] S. J. Liao and Y. Tan, "A general approach to obtain series solutions of nonlinear differential equations," *Stud. Appl. Math.*, vol. 119, pp. 297–354, 2007.
[12] S. Loghambal and L. Rajendran, "Analytical expressions of concentration of nitrate pertaining to the electrocatalytic reduction of nitrate ion," *J. Electroanal. Chem.*, vol. 661, pp. 137–143, 2011.
[13] A. Mastroberardino, "Homotopy analysis method applied to electrohydrodynamic flow," *Commun. Nonlinear Sci. Numer. Simul.*, vol. 16, pp. 2730–2736, 2011.
[14] *MATLAB 6.1*, The MathWorks Inc., Natick, MA, USA, 2000.
[15] N. J. McPherson and R. A. Norman, "Macroparasites in managed systems: Using mathematical models to help reduce the impact of *Argulus foliaceus* in UK fisheries," *Proc. Eur. Conf. Math. Theor. Biol. (ECMTB)*, 2011.
[16] N. J. McPherson, R. A. Norman, A. S. Hoyle, J. E. Bron, and N. G. H. Taylor, "Stocking methods and parasite-induced reductions in capture: Modelling *Argulus foliaceus* in trout fisheries," *J. Theor. Biol.*, vol. 312, pp. 22–33, 2012.
[17] A. Oktener, A. H. Ali, A. Gustinelli, and M. L. Fioravanti, "New host records for fish louse, *Argulus foliaceus* L., 1758 (Crustacea: Branchiura) in Turkey," *Ittiopatologia*, vol. 3, pp. 161–167, 2006.
[18] A. F. Pasternak, V. N. Micheev, and E. T. Valtonen, "Life history characteristics of *Argulus foliaceus* L. (Crustacea: Branchiura) population in Central Finland," *Ann. Zool. Fenn.*, vol. 37, pp. 25–35, 2000.
[19] M. Rasi, K. Indira, and L. Rajendran, "Approximate analytical expressions for the steady-state concentration of substrate and cosubstrate over amperometric biosensors for different enzyme kinetics," *Int. J. Chem. Kinet.*, vol. 45, pp. 322–336, 2013.
[20] R. D. Skeel and M. Berzins, "A method for the spatial discretization of parabolic equations in one space variable," *SIAM J. Sci. Stat. Comput.*, vol. 11, pp. 1–32, 1990.
[21] A. R. Sohouli, M. Famouri, A. Kimiaeifar, and G. Domairry, "Application of homotopy analysis method for natural convection of Darcian fluid about a vertical full cone embedded in porous media prescribed surface heat flux," *Commun. Nonlinear Sci. Numer. Simul.*, vol. 15, pp. 1691–1699, 2010.
[22] N. G. H. Taylor, R. Wootten, and C. Sommerville, "Using length-frequency data to elucidate the population dynamics of *Argulus foliaceus* (Crustacea: Branchiura)," *Parasitology*, vol. 136, pp. 1023–1032, 2009.

Appendix A: Basic concepts of Liao's homotopy analysis method

Consider the general nonlinear differential equation (Liao 2003):

$$N[u(x)] = 0 \tag{A.1}$$

where N denotes a nonlinear operator, x is the independent variable, and $u(x)$ is the unknown function. For simplicity, the boundary or initial conditions are not included here, as they can be incorporated following a similar procedure.

To analytically handle such nonlinear problems, Liao (2003) extended the classical homotopy concept and developed the zero-order deformation equation, a fundamental component of the HAM. This method constructs a continuous deformation from an initial approximation to the exact solution by introducing an embedding parameter, and it provides flexibility through an auxiliary parameter that controls convergence.

$$(1-p)L[\varphi(x;p) - u_0(x)] = phH(x)N[\varphi(x;p)] \tag{A.2}$$

Here, p∈[0,1 is the embedding parameter, $\hbar \neq 0$ is a nonzero auxiliary parameter, H(x) is an auxiliary function, L is an auxiliary linear operator, and $u_0(x)$ is an initial guess of the solution $u(x)$, which is the unknown function to be determined. One of the notable advantages of the HAM is the considerable freedom it offers in the selection of these auxiliary components.

By construction, when p=0 and p=1, the zero-order deformation equation satisfies:

$$\begin{cases} \phi(x;0) = u_0(x) \\ \phi(x;1) = u(x) \end{cases} \tag{A.3}$$

which ensures a continuous deformation from the initial guess $u_0(\xi)$ to the exact solution u(ξ) as the embedding parameter p varies from 0 to 1.

Thus, as the embedding parameter p increases from 0 to 1, the solution u($x;p$) continuously deforms from the initial guess $u_0(x)$ to the exact solution u(x). Expanding u($x;p$) in a Taylor series with respect to p, we obtain:

$$\varphi(x;p) = u_0(x) + \sum_{m=1}^{+\infty} u_m(x)\, p^m \tag{A.4}$$

where

$$u_m(x) = \frac{1}{m!}\frac{\partial^m \varphi(x;p)}{\partial p^m}\Big|_{p=0} \tag{A.5}$$

If the auxiliary linear operator L, the initial guess $u_0(x)$, the auxiliary parameter $\hbar$, and the auxiliary function $H(x)$ are chosen appropriately such that the series expansion (A.4) converges at p=1, then the exact solution $u(x)$ of the original nonlinear differential equation (A.1) is given by:

$$u(x) = u_0(x) + \sum_{m=1}^{+\infty} u_m(x)\,. \tag{A.6}$$

Define the vector $\vec{u} = \{u_0, u_1, \ldots, u_n\}$

Differentiating the zero-order deformation equation (A.2) mmm times with respect to the embedding parameter p, then setting p=0, and finally dividing the resulting expression by m!, we obtain the so-called m^{th}-order deformation equation:
This recursive system enables the sequential determination of $u_m(\xi)$, thereby constructing an analytic approximation to the solution of the original nonlinear problem.

$$L[u_m - \chi_m u_{m-1}] = hH(x)\Re_m(\vec{u}_{m-1}) \tag{A.8}$$

where

$$\Re_m(\vec{u}_{m-1}) = \frac{1}{(m-1)!}\frac{\partial^{m-1}N[\varphi(x;p)]}{\partial p^{m-1}} \tag{A.9}$$

and

$$\chi_m = \begin{cases} 0, & m \le 1, \\ 1, & m > 1. \end{cases} \tag{A.10}$$

Applying L^{-1} on both side of equation (A.8), we get

$$u_m(x) = \chi_m u_{m-1}(x) + hL^{-1}[H(x)\Re_m(\vec{u}_{m-1})] \tag{A.11}$$

In this way, it is easily to obtain u_m for $m \ge 1$, at M^{th} order, we have

$$u(x) = \sum_{m=0}^{M} u_m(x)$$

When the homotopy series converges at p=1, it yields an accurate approximation to the exact solution of the original nonlinear equation (A.1). For a detailed discussion on the convergence theorems and conditions of the HAM, the reader is referred to Liao (2003).

If equation (A.1) admits a unique solution, then the HAM series solution will converge to this unique solution, provided the auxiliary components are properly selected. However, if the original equation (A.1) does not possess a unique solution, HAM is still capable of yielding a valid solution though it may be one among multiple possible solutions depending on the chosen initial guess and auxiliary functions.

Appendix B: Approximate analytical solutions for Eqn. (4) - (6) using HAM
In order to solve Eqn. (4) to (6) by means of the HAM, we first construct the Zeroth-order deformation equation by taking H (t) = 1.

$$(1-p)\left\{\frac{dH}{dt} - (a-c)H\right\} = ph\left\{\frac{dH}{dt} - (a-c)H + \alpha P\right\} \tag{B.1}$$

$$(1-p)\left\{\frac{dP}{dt} + (\mu+\alpha+c)P\right\} = ph\left\{\frac{dT}{dt} - \beta HW + (\mu+\alpha+c)P + \alpha k\frac{P^2}{H}\right\} \tag{B.2}$$

$$(1-p)\left\{\frac{dW}{dt} + dW\right\} = ph\left\{\frac{dW}{dt} - \lambda P + dW + \beta HW\right\} \tag{B.3}$$

The approximate solutions of Eqn. (4) - (6) are as follows:

$$H = H_0 + pH_1 + p^2 H_2 + ... \tag{B.4}$$

$$P = P_0 + pP_1 + p^2 P_2 + ... \tag{B.5}$$

$$W = W_0 + pW_1 + p^2 W_2 + ... \tag{B.6}$$

Substituting (B.4) in Eqn. (B.1) and equating the like powers of p we get

$$p^0 : \frac{dH_0}{dt} - (a-c)H_0 = 0 \tag{B.7}$$

$$p^1 : \frac{dH_1}{dt} - (a-c)H_1 = (h+1)\left[\frac{dH_0}{dt} - (a-c)H_0\right] + h[\alpha P_0] \tag{B.8}$$

Substituting (B.5) in Eqn. (B.2) and equating the like powers of p we get

$$p^0 : \frac{dP_0}{dt} + (\mu + \alpha + c)P_0 = 0 \tag{B.9}$$

$$p^1 : \frac{dP_1}{dt} + (\mu + \alpha + c)P_1 = (h+1)\left[\frac{dP_0}{dt} + (\mu + \alpha + c)P_0\right] + h\left[-\beta H_0 W_0 + \alpha k \frac{{P_0}^2}{H_0}\right] \tag{B.10}$$

Substituting Eqn. (B.6) in Eqn. (B.2) and equating the like powers of p we get

$$p^0 : \frac{dW_0}{dt} + dW_0 = 0 \tag{B.11}$$

$$p^1 : \frac{dW_1}{dt} + dW_1 = (h+1)\left[\frac{dW_0}{dt} + dW_0\right] + h[-\lambda P_0 + H_0 W_0] \tag{B.12}$$

The initial conditions in Eqn. (7) becomes

$$H_0 = 1,\ P_0 = 1 \text{ and } W_0 = 1 \text{ when } t = 0 \tag{B.13}$$

$$H_1 = 0,\ P_1 = 0 \text{ and } W_1 = 1 \text{ when } t = 0 \tag{B.14}$$

Now applying the initial conditions (B.13) in Eqns. (B.7), (B.9) and (B.11) we get

$$H_0 = e^{(a-c)t} \tag{B.15}$$

$$P_0 = e^{-(\mu+\alpha+c)t} \tag{B.16}$$

$$W_0 = e^{-dt} \tag{B.17}$$

Substituting the values of H_0, P_0 and W_0 in Eqn. (B.8) and (B.10) and solving the equations using the initial conditions (B.14) we obtain the following results:

$$H_1 = \frac{h\alpha}{(\mu+\alpha+a)}\left[e^{(a-c)t} - e^{-(\mu+\alpha+c)t}\right] \tag{B.18}$$

$$\begin{aligned} P_1 = {} & \frac{h\beta}{(a-d+\mu+\alpha)}\left[e^{-(\mu+\alpha+c)t} - e^{(a-d-c)t}\right] \\ & + \frac{h\alpha}{(\mu+\alpha+a)}\left[e^{-(\mu+\alpha+c)t} - e^{-(2\mu+2\alpha+c+a)t}\right] \end{aligned} \tag{B.19}$$

$$W_1 = \frac{h\lambda}{(\mu+\alpha+c-d)}\left[e^{-(\mu+\alpha+c)t} - e^{-dt}\right] + \frac{h\beta}{(a-c)}\left[e^{(a-c-d)t} - e^{-dt}\right] \tag{B.20}$$

Adding Eqn. (B.15) and (B.18), we get Eqn. (9) in the text. Similarly we get Eqn. (10) and Eqn. (11) in the text.

Approximate analytical solutions for Eqn. (12), (13) and (14) using HAM

In order to solve Eqns. (12) to (14) by means of the HAM, we first construct the Zeroth- order deformation equation by taking H (t) = 1.

$$(1-p)\left\{\frac{dH}{dt} - (a-c)H\right\} = ph\left\{\frac{dH}{dt} - (a-c)H + (\alpha - c\theta)P\right\} \tag{B.21}$$

$$(1-p)\left\{\frac{dP}{dt} + (\mu+\alpha+1)P\right\} = ph\left\{\frac{dT}{dt} - \beta HW + (\mu+\alpha+1)P + (\alpha k - \theta)\frac{P^2}{H}\right\} \tag{B.22}$$

$$(1-p)\left\{\frac{dW}{dt} + dW\right\} = ph\left\{\frac{dW}{dt} - \lambda P + dW + \beta HW\right\} \tag{B.23}$$

The approximate solutions of Eqns. (12) - (14) are as follows:

$$H = H_0 + pH_1 + p^2H_2 + ... \tag{B.24}$$

$$P = P_0 + pP_1 + p^2P_2 + ... \tag{B.25}$$

$$W = W_0 + pW_1 + p^2W_2 + ... \tag{B.26}$$

Substituting (B.24) in Eqn. (B.21) and equating the like powers of p we get

$$p^0 : \frac{dH_0}{dt} - (a-c)H_0 = 0 \tag{B.27}$$

$$p^1 : \frac{dH_1}{dt} - (a-c)H_1 = (h+1)\left[\frac{dH_0}{dt} - (a-c)H_0\right] + h\left[(\alpha - c\theta)P_0\right] \tag{B.28}$$

Substituting (B.25) in Eqn. (B.22) and equating the like powers of p we get

$$p^0 : \frac{dP_0}{dt} + (\mu+\alpha+1)P_0 = 0 \tag{B.29}$$

$$p^1 : \frac{dP_1}{dt} + (\mu+\alpha+1)P_1 = (h+1)\left[\frac{dP_0}{dt} + (\mu+\alpha+1)P_0\right] + h\left[-\beta H_0W_0 + (\alpha k - \theta)\frac{{T_0}^2}{H_0}\right] \tag{B.30}$$

Substituting (B.26) in Eqn. (B.22) and equating the like powers of p we get

$$p^0 : \frac{dW_0}{dt} + dW_0 = 0 \tag{B.31}$$

$$p^1 : \frac{dW_1}{dt} + dW_1 = (h+1)\left[\frac{dW_0}{dt} + dW_0\right] + h\left[-\lambda P_0 + H_0W_0\right] \tag{B.32}$$

The initial conditions in Eqn. (7) becomes

$$H_0 = 1,\ P_0 = 1 \text{ and } W_0 = 1 \text{ when } t = 0 \tag{B.33}$$

$H_1 = 0,\ P_1 = 0$ and $W_1 = 1$ when $t = 0$ (B.34)

Now applying the initial conditions (B.33) in (B.27), (B.29) and (B.31) we get

$$H_0 = e^{(a-c)t} \tag{B.35}$$

$$P_0 = e^{-(\mu+\alpha+1)t} \tag{B.36}$$

$$W_0 = e^{-dt} \tag{B.37}$$

Substituting the values of H_0, P_0 and W_0 in Eqn. (B.28) and (B.30) and solving the equations using the initial conditions (B.34) we obtain the following results:

$$H_1 = \frac{h(\alpha - c\theta)}{(\mu + \alpha + 1 + a - c)}\left[e^{(a-c)t} - e^{-(\mu+\alpha+1)t}\right] \tag{B.38}$$

$$\begin{aligned} P_1 = {} & \frac{h\beta}{(a - c - d + \mu + \alpha + 1)}\left[e^{-(\mu+\alpha+1)t} - e^{(a-d-c)t}\right] \\ & - \frac{h(\alpha k - \theta)}{(\mu + \alpha + 1 + a - c)}\left[e^{-(\mu+\alpha+c)t} - e^{-(2\mu+2\alpha+2+a-c)t}\right] \end{aligned} \tag{B.39}$$

$$W_1 = \frac{h\lambda}{(\mu + \alpha + 1 - d)}\left[e^{-(\mu+\alpha+1)t} - e^{-dt}\right] + \frac{h\beta}{(a - c)}\left[e^{(a-c-d)t} - e^{-dt}\right] \tag{B.40}$$

Adding Eqns. (B.35) and (B.38), we get Eqn. (15) in the text. Similarly, we get Eqns. (16) and (17) in the text.